J. Fluid Mech. (1987), *vol.* 178, *pp.* 459–475
Printed in Great Britain

On nonlinear K–l and K–ϵ models of turbulence

By CHARLES G. SPEZIALE

The George W. Woodruff School of Mechanical Engineering, Georgia Institute of Technology, Atlanta, GA 30332, USA

(Received 3 March 1986 and in revised form 6 October 1986)

The commonly used linear K–l and K–ϵ models of turbulence are shown to be incapable of accurately predicting turbulent flows where the normal Reynolds stresses play an important role. By means of an asymptotic expansion, nonlinear K–l and K–ϵ models are obtained which, unlike all such previous nonlinear models, satisfy both realizability and the necessary invariance requirements. Calculations are presented which demonstrate that this nonlinear model is able to predict the normal Reynolds stresses in turbulent channel flow much more accurately than the linear model. Furthermore, the nonlinear model is shown to be capable of predicting turbulent secondary flows in non-circular ducts – a phenomenon which the linear models are fundamentally unable to describe. An additional application of this model to the improved prediction of separated flows is discussed briefly along with other possible avenues of future research.

1. Introduction

Despite the intensive research effort of the past decade to develop more general turbulence models, the linear K–l and K–ϵ models of turbulence still remain the most widely used approach by engineers and scientists for the solution of practical problems. The reason for this state of affairs becomes abundantly clear when one considers the disadvantages of the two major alternative approaches, namely second-order closure models and large-eddy simulations. For second-order closure models, the computational effort is more than doubled since transport equations must be solved for each individual component of the Reynolds stress tensor (cf. Launder, Reece & Rodi 1975; Mellor & Herring 1973; Lumley 1978). Furthermore, in order to obtain these transport equations for the Reynolds stresses, closure models for the higher-order turbulence correlations must be provided which have uncertain physical foundations. It is the opinion of many turbulence researchers that these deficiencies outweigh the main advantage of second-order closures, namely the incorporation of history-dependent non-local effects (through the convection and viscous diffusion of the Reynolds stresses) which are known to play an important role in determining the structure of many turbulent flows. Large-eddy simulations, by their nature, constitute three-dimensional time-dependent computations that require enormous computer time in comparison to the more traditional turbulent closure models. Furthermore, as a result of difficulties in modelling the turbulence in the vicinity of solid boundaries (cf. Deardorff 1970; Moin & Kim 1982) and the problem of defiltering the results in complex geometries, this approach is still not suitable for the solution of many problems of technological importance. Since the linear K–ϵ and K–l models reduce to the mixing length theories for thin shear flows (in fact, these models can be thought of as tensorially invariant mixing length theories) they usually do quite well in the description of unseparated turbulent boundary layers which form a cornerstone for many engineering problems. This result, along with the fact that the K–ϵ and K–l models can be incorporated into most Navier–Stokes computer codes in a relatively simple manner, constitute the main reasons for the continued popularity of this approach.

It is well known that the linear K–l and K–ϵ models of turbulence can give rise to highly inaccurate predictions for the normal Reynolds stresses which make it impossible to describe such effects as secondary flows in non-circular ducts (see Launder & Ying 1971; Gessner & Emery 1976; Speziale 1982, 1984). Consequently, there have been previous research efforts to generalize these models to include nonlinear effects (see Lumley 1970; Launder & Ying 1971; Gessner & Emery 1976; Saffman 1977; Rodi 1982). However, these models were developed in a somewhat preliminary fashion and, as will be seen herein, do not exhibit the general invariance which is necessary if the broadest possible range of applicability is to be achieved. The purpose of the present paper is to develop, in a systematic manner, nonlinear K–l and K–ϵ models of turbulence which will broaden the range of validity of the more traditional models while maintaining most of their popular features (i.e. reduction to the mixing-length theories for thin shear flows and the ease of application in existing Navier–Stokes computer codes without substantially raising the level of computation). This will be accomplished by making an asymptotic expansion subject to the constraints of dimensional and tensorial invariance, realizability and material frame-indifference in the limit of two-dimensional turbulence which are a rigorous consequence of the Navier–Stokes equations. The resulting nonlinear model that will be obtained has a structure similar to that of a Rivlin–Ericksen fluid which is used in the description of the flows of dilute polymer solutions and, furthermore, constitutes a special case of the more complex nonlinear eddy viscosity model obtained by Yoshizawa (1984) using Kraichnan's DIA formalism. It has long been known that there are striking similarities between the mean turbulent flow of a Newtonian fluid and the laminar flow of viscoelastic fluids, which motivated Rivlin (1957) and Lumley (1970) to suggest the use of viscoelastic models in turbulence.

The nonlinear K–l and K–ϵ models that are obtained in this study will be shown to yield drastically improved predictions for the normal Reynolds stresses in turbulent channel flow and to yield normal-Reynolds-stress differences that give rise to secondary flows in non-circular ducts (preliminary computations for fully developed turbulent flow in a square duct will be presented). An additional application of this nonlinear model to the improved prediction of separated turbulent flows will also be discussed along with the prospects for future research.

2. Linear K–l and K–ϵ models

The mean turbulent flow of an incompressible and homogeneous viscous fluid will be considered for which the velocity field $\boldsymbol{v}$ and pressure field P can be decomposed into ensemble mean and fluctuating parts, respectively, as follows:

$$\boldsymbol{v} = \bar{\boldsymbol{v}} + \boldsymbol{u}, \quad P = \bar{P} + p. \tag{1}$$

The evolution of $\bar{\boldsymbol{v}}$ and $\bar{P}$ in time are governed by the Reynolds equation and continuity equation which take form (cf. Hinze 1975)

$$\rho\left(\frac{\partial \bar{\boldsymbol{v}}}{\partial t} + \bar{\boldsymbol{v}}\cdot\nabla\bar{\boldsymbol{v}}\right) = -\nabla\bar{P} + \rho\boldsymbol{F} + \mu\nabla^2\bar{\boldsymbol{v}} + \nabla\cdot\boldsymbol{\tau}, \tag{2}$$

$$\nabla\cdot\bar{\boldsymbol{v}} = 0, \tag{3}$$

where $\boldsymbol{\tau}$ is the Reynolds stress tensor whose components are given by

$$\tau_{ij} = -\rho\overline{u_i u_j}, \tag{4}$$

ρ is the density of the fluid, μ is the dynamic viscosity of the fluid, and $\boldsymbol{F}$ is the external body force per unit mass. Of course, it is well known that as a result of the additional unknowns represented by $\boldsymbol{\tau}$, the equations of motion (2)–(3) for the evolution of the mean turbulent fields are not closed. Closure is usually achieved by providing equations where the Reynolds stress tensor is tied to the global history of the mean velocity field. More specifically, it is assumed that

$$\boldsymbol{\tau}(\boldsymbol{x},t) = \boldsymbol{\tau}[\overline{\boldsymbol{v}}(\boldsymbol{x}',t');\boldsymbol{x},t], \quad \boldsymbol{x}'\in D, \quad t'\in(-\infty,t), \tag{5}$$

where the bracket denotes a functional (i.e. any quantity determined by a function) and D represents the fluid domain.

In the linear K–l model of turbulence the Reynolds stress tensor is taken to be of the form

$$\tau_{ij} = -\tfrac{2}{3}\rho K\delta_{ij} + \rho K^{\frac{1}{2}} l \overline{D}_{ij}, \tag{6}$$

where

$$K = -\frac{1}{2\rho}\tau_{jj}, \tag{7}$$

$$\overline{D}_{ij} = \frac{1}{2}\left(\frac{\partial \overline{v}_i}{\partial x_j} + \frac{\partial \overline{v}_j}{\partial x_i}\right) \tag{8}$$

are, respectively, the turbulent kinetic energy per unit mass and the mean rate of strain tensor, while l denotes the lengthscale of turbulence. The turbulent kinetic energy is obtained from a modelled version of its transport equation, which can take the form (cf. Mellor & Herring 1973)

$$\frac{\mathrm{D}K}{\mathrm{D}t} = \nu\nabla^2 K + \alpha_1\frac{\partial}{\partial x_i}\left(K^{\frac{1}{2}} l\frac{\partial K}{\partial x_i}\right) + \frac{1}{\rho}\tau_{ij}\frac{\partial \overline{v}_j}{\partial x_i} - \alpha_2\frac{K^{\frac{3}{2}}}{l}, \tag{9}$$

where $\mathrm{D}/\mathrm{D}t = \partial/\partial t + \overline{\boldsymbol{v}}\cdot\nabla$ and α_1 and α_2 are dimensionless constants. The lengthscale of turbulence in the K–l model is either specified algebraically by empirical means for simple turbulent flows (e.g. unseparated turbulent boundary layers), or it can be obtained from a transport equation which is constructed from a modelled version of the contracted form of the evolution equation for the two-point double velocity correlations (cf. Mellor & Herring 1973). This transport equation for the lengthscale takes the form

$$\frac{\mathrm{D}(Kl)}{\mathrm{D}t} = \frac{\partial}{\partial x_i}\left[(\nu+\beta_1 K^{\frac{1}{2}} l)\frac{\partial}{\partial x_i}(Kl) + \beta_2 K^{\frac{3}{2}} l\frac{\partial l}{\partial x_i}\right] + \beta_3\frac{l}{\rho}\tau_{ij}\frac{\partial \overline{v}_i}{\partial x_j} - \beta_4 K^{\frac{3}{2}}, \tag{10}$$

where $\beta_1, \ldots, \beta_4$ are dimensionless constants.

In the K–ϵ model, the lengthscale of turbulence is taken to be of the form

$$l = C\frac{K^{\frac{3}{2}}}{\epsilon}, \tag{11}$$

where

$$\epsilon = \nu\overline{\frac{\partial u_i}{\partial x_j}\frac{\partial u_i}{\partial x_j}} \tag{12}$$

is the dissipation rate of the turbulence and C is a dimensionless constant. Here, the turbulent kinetic energy K and dissipation rate ϵ are obtained from modelled versions of their transport equations which can take a variety of forms. In the Launder model (cf. Hanjalic & Launder 1972) these transport equations are, at high Reynolds numbers, as follows:

$$\frac{\mathrm{D}K}{\mathrm{D}t} = \frac{1}{\rho}\tau_{ij}\frac{\partial \bar{v}_i}{\partial x_j} + C_1\frac{\partial}{\partial x_i}\left[\frac{K}{\rho^2\epsilon}\left(\tau_{jm}\frac{\partial \tau_{ij}}{\partial x_m} - \rho\tau_{ij}\frac{\partial K}{\partial x_j}\right)\right] - \epsilon, \tag{13}$$

$$\frac{\mathrm{D}\epsilon}{\mathrm{D}t} = -\frac{C_2}{\rho}\frac{\partial}{\partial x_i}\left(\frac{K}{\epsilon}\tau_{ij}\frac{\partial \epsilon}{\partial x_j}\right) + C_3\frac{\epsilon}{\rho K}\tau_{ij}\frac{\partial \bar{v}_i}{\partial x_j} - C_4\frac{\epsilon^2}{K}, \tag{14}$$

where $C_1, \ldots, C_4$ are dimensionless constants.

As a result of the simplicity of its structure, the K–l (or K–ϵ) model does have certain advantages. Since it actually constitutes a tensorially invariant eddy-viscosity model (with eddy viscosity $\frac{1}{2}\rho K^{\frac{1}{2}}l$), it can easily be incorporated into any existing Navier–Stokes computer code which allows for a variable viscosity. It does extremely well in the analysis of thin turbulent shear flows since it reduces to the traditional eddy-viscosity models which were constructed for this purpose. Furthermore, this model is frame-indifferent (i.e. is of the same form whether or not the frame of reference is inertial). Consequently, the principle of material frame-indifference in the limit of two-dimensional turbulence, which is a rigorous consequence of the Navier–Stokes equations (see Speziale 1981, 1983), is satisfied identically.

Although the ease of application of the K–ϵ and K–l models (along with its accuracy in the calculation of thin turbulent shear flows) are very positive features, these models nevertheless yield inaccurate predictions for the normal Reynolds stresses. Consequently, flows where the normal Reynolds stresses play an important role (e.g. problems involving recirculation and secondary flows) cannot be calculated properly with the linear K–ϵ or K–l model. While this point has been briefly alluded to previously in the literature, it will now be demonstrated in more detail. To begin with, it is well known that the K–ϵ and K–l models predict that the normal Reynolds stresses in a fully developed turbulent channel flow (see figure 1) are all equal – a result which is in substantial contradiction of experiments. This erroneous equality of the normal Reynolds stresses is also predicted by the K–ϵ and K–l models when applied to the problem of fully developed turbulent flow in a non-circular duct (see figure 2). Since the K–ϵ and K–l models predict that

$$\tau_{yy} = \tau_{xx}, \tag{15}$$

they yield unidirectional mean turbulent flows in non-circular ducts which is in contradiction of experiments that demonstrate the presence of secondary flows as illustrated in figure 2. It has been proven that in order for secondary flows to occur, the axial mean velocity must give rise to a non-zero transverse normal-Reynolds-stress difference $\tau_{yy} - \tau_{xx}$ (cf. Speziale 1982, 1984).

In addition to being incapable of describing secondary flows in non-circular ducts, the K–ϵ and K–l models given by (6) give rise to substantial inaccuracies in the calculation of separated turbulent flows. In particular, for turbulent flow over a backward-facing step (see figure 3), the K–ϵ and K–l models yield inaccurate values for the separation length L and for the normal Reynolds stresses. The reason for this difficulty becomes clear if one considers an arbitrary two-dimensional mean turbulent flow of the form

$$\bar{\boldsymbol{v}} = \bar{u}(x,y)\,\boldsymbol{i} + \bar{v}(x,y)\boldsymbol{j}. \tag{16}$$

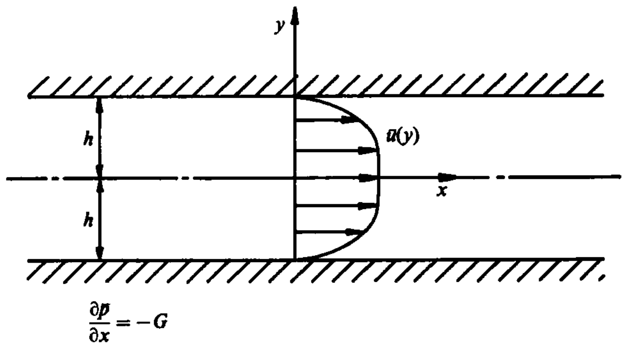

FIGURE 1. Fully developed turbulent channel flow.

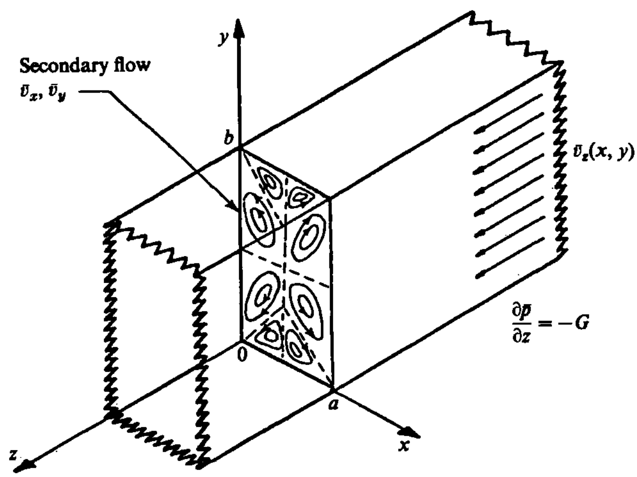

FIGURE 2. Fully developed turbulent flow in a rectangular duct.

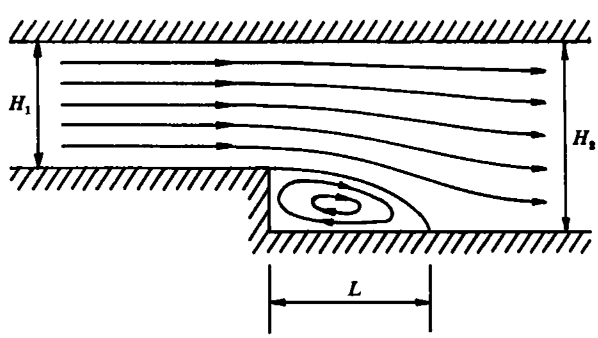

FIGURE 3. Turbulent separated flow over a backward-facing step.

For such a flow, the K–l (or K–ϵ) model defined by (6) predicts that

$$\tau_{xx}+\tau_{yy} = 2\tau_{zz} \tag{17}$$

for all choices of $\bar{u}$ and $\bar{v}$. Clearly, this is not true in general and can lead to significant errors in the calculation of the normal Reynolds stresses. These errors are not significant in the calculation of thin turbulent shear flows since, for such flows, the normal Reynolds stresses do not enter into the calculation of the mean velocity. However, for a separated flow such as that shown in figure 3, the normal Reynolds stresses play an important rôle in the calculation of the mean velocity field through the terms $\partial \tau_{xx}/\partial x$ and $\partial \tau_{yy}/\partial y$.

It will be shown in the next section that these inaccuracies in the predictions for the normal Reynolds stresses can be alleviated by the addition of nonlinear terms of an invariant form. Hopefully, then it will become possible to analyse secondary flows and recirculating flows without the need for *ad hoc* empiricisms.

3. Nonlinear K–l and K–ϵ models

In order to develop nonlinear turbulence models which transcend the linear K–l and K–ϵ models, but are not considerably more complex in structure, we shall restrict our attention to algebraic models that are quadratic in the mean velocity gradients – the next highest approximation to (6). However, it should be noted that terms that are quadratic in $\nabla \bar{\boldsymbol{v}}$ are of the same dimensions as terms that are linear in $\mathrm{D}(\nabla \bar{\boldsymbol{v}})/\mathrm{D}t$. Hence, for consistency, time derivatives of $\nabla \bar{\boldsymbol{v}}$ must be included along with nonlinear terms in $\nabla \bar{\boldsymbol{v}}$ (the same situation occurs in the kinetic theory of gases when asymptotic solutions to the Boltzmann equation are obtained; cf. Chapman & Cowling 1953). Of course, in order to keep the same general theoretical framework as in the linear K–ϵ and K–l models, $\boldsymbol{\tau}$ will be allowed to depend on K and l which will be obtained from separate transport equations. Thus, the following functional form is assumed for the Reynolds stress tensor:

$$\boldsymbol{\tau} = \boldsymbol{\tau}\left[\nabla \bar{\boldsymbol{v}}, \frac{\mathrm{D}(\nabla \bar{\boldsymbol{v}})}{\mathrm{D}t}, K, l, \rho\right], \tag{18}$$

where, for dimensional consistency, a parametric dependence on the density ρ needs to be included. There are several powerful constraints that can be invoked in order to simplify the structure of the quadratic theory obtained from (18) and to guarantee consistency with certain general properties of the Navier–Stokes equations:

(i) general coordinate and dimensional invariance;

(ii) realizability (i.e. positiveness of the turbulent kinetic energy,† see Lumley 1978);

(iii) material frame – indifference in the limit of two-dimensional turbulence (see Speziale 1981, 1983).

Constraint (i) is satisfied identically by casting the model in tensor form and by making sure that all model constants are dimensionless (this latter condition guarantees similitude under the Reynolds number – a general property of all solutions of the Navier–Stokes equations). Constraint (ii) can be satisfied by taking

$$\tau_{ij} = -\tfrac{2}{3}\rho K \delta_{ij} + {}_{\mathrm{D}}\tau_{ij}, \tag{19}$$

where ${}_{\mathrm{D}}\boldsymbol{\tau}$ is a traceless tensor and the transport equation for the turbulent kinetic energy is formulated in such a way that $K > 0$ (cf. Lumley 1978 for the details of how this is achieved). The last constraint places the most powerful restrictions on the allowable form of (18). It arises as a rigorous consequence of the two-dimensional

† This constitutes the same realizability, in the weak sense, that the linear K–ϵ and K–l models are only known to satisfy (full realizability requires each component of the energy, i.e. $-\tau_{xx}/\rho$, $-\tau_{yy}/\rho$, $-\tau_{zz}/\rho$, to be positive for any possible flow).

Navier–Stokes equations which are approached by any turbulence in a rapidly rotating framework that is sufficiently far from solid boundaries (a direct result of the Taylor–Proudman theorem; see Speziale 1981, 1985). In mathematical terms, constraint (iii) requires that the closure relation (18) in a two-dimensional turbulence be form-invariant under a change of frame, i.e. (18) must be of the same form

$$\boldsymbol{\tau}^* = \boldsymbol{\tau}\left[\nabla^*\bar{\boldsymbol{v}}^*, \frac{\mathrm{D}(\nabla\bar{\boldsymbol{v}})^*}{\mathrm{D}t^*}, K^*, l^*, \rho\right] \tag{20}$$

in all non-inertial frames of reference $\boldsymbol{x}^*$ which can undergo arbitrary time-dependent rotations and translations relative to an inertial framing. Under a change of frame, the mean velocity gradients transform as

$$\nabla^*\bar{\boldsymbol{v}}^* = \nabla\bar{\boldsymbol{v}} + \mathrm{dual}\,\boldsymbol{\Omega}, \tag{21}$$

where dual $\boldsymbol{\Omega}$ is the antisymmetric tensor formed from the angular velocity $\boldsymbol{\Omega}$ of the non-inertial framing as follows:

$$(\mathrm{dual}\,\boldsymbol{\Omega})_{ij} = \epsilon_{ijk}\,\Omega_k, \tag{22}$$

given that ϵ_{ijk} is the permutation tensor. Hence, $\nabla\bar{\boldsymbol{v}}$ is a frame-dependent tensor which is non-zero in a two-dimensional turbulence. Of course, the turbulent kinetic energy K and the lengthscale of turbulence l are frame-indifferent scalars, i.e. they transform as

$$K^* = K, \quad l^* = l \tag{23}$$

under a change of frame (cf. Speziale 1983). Consequently, any polynomial approximation to (18) must be constructed from the frame-indifferent parts of $\nabla\bar{\boldsymbol{v}}$ and $\mathrm{D}(\nabla\bar{\boldsymbol{v}})/\mathrm{D}t$ in order to satisfy constraint (iii). These frame-indifferent parts of $\nabla\bar{\boldsymbol{v}}$ and $\mathrm{D}(\overline{\nabla}\boldsymbol{v})/\mathrm{D}t$ are, respectively, as follows (cf. Speziale 1983):

$$\bar{D}_{ij} = \frac{1}{2}\left(\frac{\partial\bar{v}_i}{\partial x_j} + \frac{\partial\bar{v}_j}{\partial x_i}\right), \tag{24}$$

$$\overset{\circ}{\bar{D}}_{ij} = \frac{\partial\bar{D}_{ij}}{\partial t} + \bar{\boldsymbol{v}}\cdot\nabla\bar{D}_{ij} - \frac{\partial\bar{v}_i}{\partial x_k}\bar{D}_{kj} - \frac{\partial\bar{v}_j}{\partial x_k}\bar{D}_{ki}, \tag{25}$$

where $\overset{\circ}{\bar{\boldsymbol{D}}}$ is the frame-indifferent Oldroyd derivative of $\bar{\boldsymbol{D}}$. Under an arbitrary change of frame,

$$\bar{\boldsymbol{D}}^* = \bar{\boldsymbol{D}}, \tag{26}$$

$$\overset{\circ}{\bar{\boldsymbol{D}}}{}^* = \overset{\circ}{\bar{\boldsymbol{D}}} \tag{27}$$

and, thus, they are invariant. Hence, we must take

$$\tau_{ij} = -\tfrac{2}{3}\rho K\delta_{ij} + {}_{\mathrm{D}}\tau_{ij}[\bar{\boldsymbol{D}}, \overset{\circ}{\bar{\boldsymbol{D}}}, K, l, \rho], \tag{28}$$

where ${}_{\mathrm{D}}\tau_{ii} = 0$. Since $\overset{\circ}{\bar{\boldsymbol{D}}}$ is quadratic in the mean velocity gradients, it is clear that the linear approximation to (28) is the standard K–l model given by equation (6). Here, we are interested in the next higher approximation to (28) – namely the quadratic theory in the mean velocity gradients. This simple nonlinear representation for $\boldsymbol{\tau}$ takes the form

$$\tau_{ij} = -\tfrac{2}{3}\rho K\delta_{ij} + \rho K^{\frac{1}{2}} l\bar{D}_{ij} + \gamma_1(\bar{D}_{im}\bar{D}_{mj} - \tfrac{1}{3}\bar{D}_{mn}\bar{D}_{mn}\delta_{ij}) + \gamma_2(\overset{\circ}{\bar{D}}_{ij} - \tfrac{1}{3}\overset{\circ}{\bar{D}}_{mm}\delta_{ij}), \tag{29}$$

where

$$\gamma_i = \gamma_i(K, l, \rho), \quad i = 1, 2, \tag{30}$$

and we have made use of the fact that ${}_{D}\tau_{ii} = 0$. Dimensional invariance (i.e. constraint (i)) requires that

$$\gamma_1 = C_D \rho l^2, \tag{31}$$

$$\gamma_2 = C_E \rho l^2, \tag{32}$$

where C_D and C_E are dimensionless constants. Equivalently, the lowest-order nonlinear K–ϵ model takes the form

$$\tau_{ij} = -\tfrac{2}{3}\rho K \delta_{ij} + \rho K^{\frac{1}{2}} l \overline{D}_{ij} + C_D \rho l^2 (\overline{D}_{im}\overline{D}_{mj} - \tfrac{1}{3}\overline{D}_{mn}\overline{D}_{mn}\delta_{ij}) + C_E \rho l^2 (\overset{\circ}{\overline{D}}_{ij} - \tfrac{1}{3}\overset{\circ}{\overline{D}}_{mm}\delta_{ij}), \tag{33}$$

where

$$l = C\frac{K^{\frac{3}{2}}}{\epsilon}.$$

It should be noted, of course, that as a result of (26) and (27), these nonlinear K–l and K–ϵ models are of the same form in all frames of reference independent of whether or not they are inertial. Furthermore, (33) must be supplemented with transport equations for K and ϵ that are of the same general form as (13) and (14).

It is clear that this nonlinear K–l (and K–ϵ) model differs from its linear version by the addition of two terms which are quadratic in the mean velocity gradients. In the next section, it will be demonstrated that these nonlinear terms allow for the more accurate calculation of normal-Reynolds-stress effects. However, before presenting these results, it would be of value to briefly discuss how the proposed nonlinear K–l and K–ϵ models (33) compare with previous work. It should first be mentioned that the nonlinear terms in (29), when γ_1 and γ_2 are constants, are analogous to the viscoelastic terms in the second-order Rivlin–Ericksen fluid which has been used in the analysis of dilute polymer solutions (cf. Truesdell & Noll 1965). Rivlin (1957) recognized many of the similarities between the mean turbulent flow of a Newtonian fluid and the laminar flow of a viscoelastic fluid and actually suggested that a turbulent constitutive theory for the Reynolds stresses be constructed based on $\overline{\boldsymbol{D}}$ and $\boldsymbol{A}_2$ – the second Rivlin–Ericksen tensor which is an alternate representation for $\overset{\circ}{\overline{\boldsymbol{D}}}$. Unfortunately, Rivlin never carried out these ideas. Several researchers have considered representations for the Reynolds stresses that are algebraically nonlinear in the mean velocity gradients in order to describe turbulent secondary flows in non-circular ducts (see Launder & Ying 1971; Gessner & Emery 1976; Gessner & Po 1977; Rodi 1982). However, these models were not cast in an invariant form (i.e. in order to obtain an algebraic form, several geometry-dependent assumptions such as the existence of fully developed flow had to be made) and therefore, could not be applied to a variety of different flow configurations without the need for *ad hoc* empiricisms. In an interesting paper, Lumley (1970) proposed a nonlinear constitutive equation for the Reynolds stress tensor which had a somewhat similar structure to (33). While this model was never fully tested, there are doubts as to whether it could be applied to strong turbulent shear flows since it is in violation of the principle of material frame-indifference in the limit of two-dimensional turbulence (it contains terms in the antisymmetric part of $\nabla\overline{\boldsymbol{v}}$). Such problems would be expected because of the equivalence of the effects of homogeneous antisymmetric shear and rigid-body rotations. The same criticism can be levelled against a rather interesting Reynolds-stress relaxation model proposed by Saffman (1977). Finally, and perhaps most importantly, it should be noted that the nonlinear K–l (and K–ϵ) model derived herein is a special case of a much more complex nonlinear eddy-viscosity model derived recently by Yoshizawa (1984) using Kraichnan's DIA formalism. It is quite encouraging that the additional nonlinear terms on the right-hand side of (33) can be obtained from the Navier–Stokes equations in a deductive manner.

4. Application of the nonlinear model to turbulent channel and duct flows

In order to provide a preliminary test of the nonlinear K–l model, we shall consider the problem of fully developed turbulent channel flow. A viscous fluid undergoes a turbulent flow between two parallel planes of infinite extent under the action of a constant axial pressure gradient

$$\frac{\partial \bar{P}}{\partial x} = -G \tag{34}$$

(see figure 1). The fully developed mean velocity field takes the form

$$\bar{\boldsymbol{v}} = \bar{u}(y)\,\boldsymbol{i}, \tag{35}$$

and the Reynolds stress tensor has the structure

$$\boldsymbol{\tau} = \begin{bmatrix} \tau_{xx}(y) & \tau_{xy}(y) & 0 \\ \tau_{xy}(y) & \tau_{yy}(y) & 0 \\ 0 & 0 & \tau_{zz}(y) \end{bmatrix}. \tag{36}$$

The Reynolds equation (2) yields the primary constraint on the flow

$$\mu \frac{\mathrm{d}^2\bar{u}}{\mathrm{d}y^2} + \frac{\mathrm{d}\tau_{xy}}{\mathrm{d}y} = -G. \tag{37}$$

Equation (37) is obtained from the x-component of (2) after substituting (34)–(36) and neglecting the effect of body forces. Here, the Reynolds shear stress τ_{xy} in the nonlinear K–l model (33) takes the form

$$\tau_{xy} = \tfrac{1}{2}\rho K^{\frac{1}{2}} l \frac{\mathrm{d}\bar{u}}{\mathrm{d}y}, \tag{38}$$

which is obtained by substituting (35) into (33). The transport equations for K and l take the form

$$\nu \frac{\mathrm{d}^2 K}{\mathrm{d}y^2} + \alpha_1 \frac{\mathrm{d}}{\mathrm{d}y}\left(K^{\frac{1}{2}} l \frac{\mathrm{d}K}{\mathrm{d}y}\right) + \frac{1}{\rho}\tau_{xy}\frac{\mathrm{d}\bar{u}}{\mathrm{d}y} - \alpha_2 \frac{K^{\frac{3}{2}}}{l} = 0, \tag{39}$$

$$\frac{\mathrm{d}}{\mathrm{d}y}\left[(\nu + \beta_1 K^{\frac{1}{2}} l)\frac{\mathrm{d}(Kl)}{\mathrm{d}y} + \beta_2 K^{\frac{3}{2}} l \frac{\mathrm{d}l}{\mathrm{d}y}\right] + \beta_3 \frac{l}{\rho}\tau_{xy}\frac{\mathrm{d}\bar{u}}{\mathrm{d}y} - \beta_4 K^{\frac{3}{2}} = 0 \tag{40}$$

respectively, which must be solved along with (37) and (38) subject to the appropriate boundary conditions. This allows for the determination of $\bar{u}$, K, l and τ_{xy}.

It should be noted that (38)–(40) are identical with those obtained from the linear K–l model. This is an acceptable state of affairs since the linear K–l model yields good results for the mean velocity, Reynolds shear stress, and turbulent kinetic energy (sufficiently far from the walls) in a turbulent channel flow. The problem with the linear K–l (and K–ϵ) model is in its inability to accurately predict the individual normal Reynolds stresses τ_{xx}, τ_{yy} and τ_{zz}. It will now be shown that the nonlinear

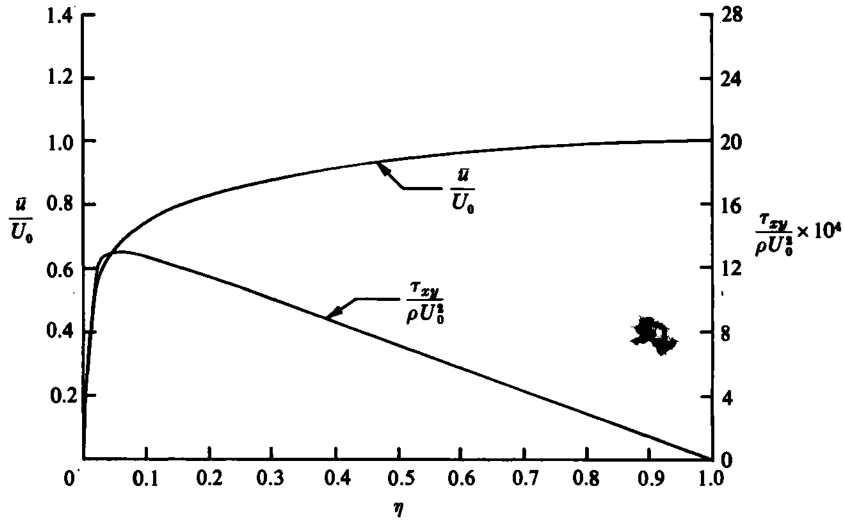

FIGURE 4. Experimental results of Laufer (1951) for fully developed turbulent channel flow. $Re = 30800$.

K–l model alleviates this problem. For turbulent channel flow, the nonlinear K–l model (33) yields the following expressions for the normal Reynolds stresses:

$$\tau_{xx} = -\tfrac{2}{3}\rho K + (\tfrac{1}{12}C_D - \tfrac{2}{3}C_E)\rho l^2 \left(\frac{d\bar{u}}{dy}\right)^2, \tag{41}$$

$$\tau_{yy} = -\tfrac{2}{3}\rho K + (\tfrac{1}{12}C_D + \tfrac{1}{3}C_E)\rho l^2 \left(\frac{d\bar{u}}{dy}\right)^2, \tag{42}$$

$$\tau_{zz} = -\tfrac{2}{3}\rho K - (\tfrac{1}{6}C_D - \tfrac{1}{3}C_E)\rho l^2 \left(\frac{d\bar{u}}{dy}\right)^2, \tag{43}$$

and, hence, $\tau_{xx} \neq \tau_{yy} \neq \tau_{zz}$ – a result which is consistent with experimental observations. In contrast to this result, the linear K–l (and K–ϵ) model yields the physically incorrect expression

$$\tau_{xx} = \tau_{yy} = \tau_{zz} = -\tfrac{2}{3}\rho K. \tag{44}$$

As stated earlier, both the linear and nonlinear K–l models yield the same predictions for the turbulent kinetic energy K, lengthscale l, and mean velocity $\bar{u}$ in turbulent channel flow (and the transport equations (39)–(40) have been demonstrated to yield accurate predictions for these quantities in the interior of the channel). Consequently, a fair basis of comparison is established between the nonlinear and linear model if the values of K, l and $d\bar{u}/dy$ are taken from experimental data and then used to calculate the individual normal Reynolds stresses using (41)–(43) and (44). The experimental data of Laufer (1951) will be used for this purpose. It is true that the experimental data of Hussain & Reynolds (1975) is generally more accurate. However, sufficiently far from the channel walls, the difference is not really that substantial and the data of Laufer (1951) is somewhat easier to make use of. The Reynolds shear stress and mean velocity obtained experimentally by Laufer are shown in figure 4 for a Reynolds number $Re = 30800$ where U_0 is the centreline mean velocity and the dimensionless variable η is defined by (see figure 1)

$$\eta = 1 - \frac{y}{h}. \tag{45}$$

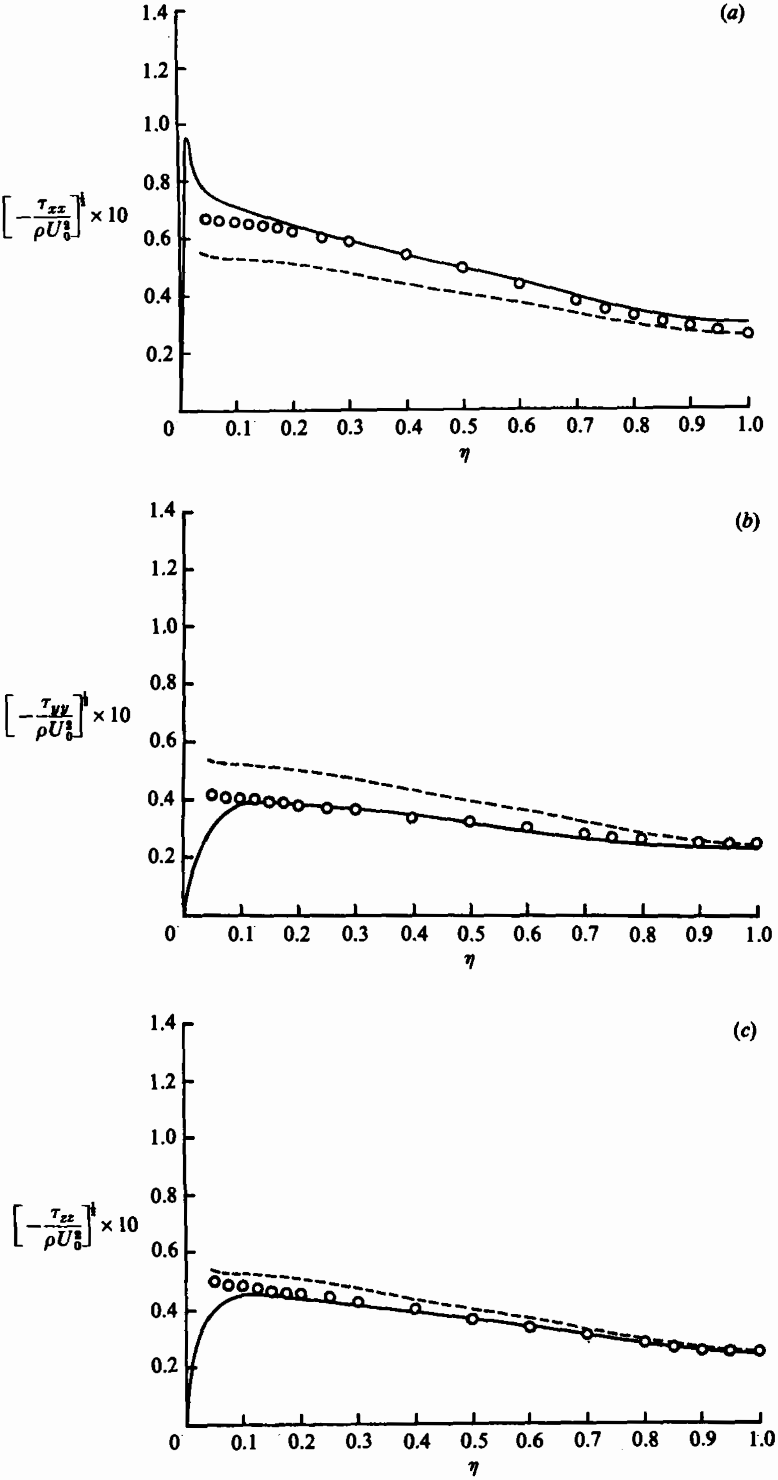

FIGURE 5. Normal Reynolds stress in turbulent channel flow: comparison of theory and experiments for $Re = 30800$. (*a*) τ_{xx}; (*b*) τ_{yy}; (*c*) τ_{zz}: ——, experimental (Laufer 1951); ○, nonlinear theory; – – – – –, linear theory.

In order to avoid complicating this figure, the turbulent kinetic energy obtained experimentally by Laufer is not shown (rather, the experimental values of $(\frac{2}{3}K/U_0^2)^{\frac{1}{2}}$, which are equivalent to the dimensionless r.m.s. values of τ_{xx}, τ_{yy} and τ_{zz} predicted by the linear K–l model for this turbulent kinetic energy, will be shown in figure 5(*a–c*)). The lengthscale of the turbulence can be obtained from τ_{xy}, K and $\bar{u}$ using (38), i.e.

$$l = \frac{2\tau_{xy}}{\rho K^{\frac{1}{2}} \mathrm{d}\bar{u}/\mathrm{d}y}. \tag{46}$$

Of course, the empirical constants C_D and C_E must be evaluated before the individual normal Reynolds stresses can be computed. From (41)–(43) it is clear that the first normal-Reynolds-stress difference $\tau_{xx} - \tau_{yy}$ only contains the constant C_E and the second normal-Reynolds-stress difference $\tau_{yy} - \tau_{zz}$ only contains the constant C_D. By making use of just one data point for these normal-Reynolds-stress differences from the experimental data of Laufer (1951) (the point $\eta = 0.5$ in the interior of the channel was considered), the constants C_D and C_E can be evaluated. These calculations yield the results

$$C_D \doteq C_E \doteq 1.68, \tag{47}$$

and, hence, there is only one additional independent constant present in this nonlinear model. Now, the individual normal Reynolds stresses can be calculated, for both the linear and nonlinear model, corresponding to the case of $Re = 30800$ discussed above. Here, the same experimental values of K, l and $\bar{u}$ obtained by Laufer (1951) are used in the calculation of the normal Reynolds stresses for both the nonlinear and the linear K–l models. These calculations, which are shown in figure 5(*a–c*), clearly demonstrate that the nonlinear K–l model yields much more accurate results for the normal Reynolds stresses than those predicted by the linear model. In fact, outside the near-wall region (i.e. for $\eta > 0.1$) the results for the nonlinear model are in almost perfect agreement with the experimental data (of course, as a result of its underlying assumptions, a K–l or K–ϵ model would not be expected to be valid in close proximity to a solid boundary). These results are quite encouraging since they were obtained by the addition of only one independent empirical constant to what appears in the linear K–l or K–ϵ models.

It will now be demonstrated that the nonlinear K–l and K–ϵ models, unlike the linear models, give rise to secondary flows in non-circular ducts – a physical effect that has been observed experimentally (cf. Gessner & Jones 1965). The necessary condition that closure models for the Reynolds stress tensor need to satisfy in order for such secondary flows to occur is as follows (see Speziale 1984): the axial mean velocity must give rise to a non-zero transverse normal-Reynolds-stress difference $\tau_{yy} - \tau_{xx}$. In the linear K–l and K–ϵ models, the axial mean velocity $\bar{v}_z$ (see figure 2) gives rise to the transverse normal-Reynolds-stress difference

$$\tau_{yy} - \tau_{xx} = 0, \tag{48}$$

which is obtained by substituting the mean velocity field $\bar{\boldsymbol{v}} = \bar{v}_z \boldsymbol{k}$ into (6) and then differencing the yy- and xx-components. Hence, the linear K–l and K–ϵ models are in violation of the necessary condition for the development of secondary flows no matter what choice is made for K, l, or ϵ. Consequently, all such linear models predict that there are unidirectional mean turbulent flows in non-circular ducts – a result which is in contradiction of experimental observations.

It will soon be seen that the nonlinear K–l model rectifies this problem. In the nonlinear K–l model, the axial mean velocity $\bar{v}_z$ gives rise to the transverse normal-Reynolds-stress difference

$$\tau_{yy}-\tau_{xx} = \tfrac{1}{4}C_D\rho l^2\left[\left(\frac{\partial \bar{v}_z}{\partial y}\right)^2-\left(\frac{\partial \bar{v}_z}{\partial x}\right)^2\right], \tag{49}$$

which, in general, is non-zero and hence satisfies the necessary condition for the development of secondary flows. Here, (49) is obtained by substituting $\bar{\boldsymbol{v}} = \bar{v}_z\boldsymbol{k}$ into (33) and then differencing the yy- and xx-components. Likewise, the axial mean velocity $\bar{v}_z$ gives rise to the Reynolds shear stresses

$$\tau_{xy} = \tfrac{1}{4}C_D\rho l^2\frac{\partial \bar{v}_z}{\partial x}\frac{\partial \bar{v}_z}{\partial y}, \tag{50}$$

$$\tau_{xz} = \tfrac{1}{2}\rho K^{\frac{1}{2}}l\frac{\partial \bar{v}_z}{\partial x}, \tag{51}$$

$$\tau_{yz} = \tfrac{1}{2}\rho K^{\frac{1}{2}}l\frac{\partial \bar{v}_z}{\partial y}. \tag{52}$$

Equations (49)–(52) represent good approximations for $\tau_{yy}-\tau_{xx}$, τ_{xy}, τ_{xz} and τ_{yz} since, for turbulent flow in a non-circular duct, the magnitude of the secondary flow is only approximately one percent of that of the axial flow (cf. Gessner & Jones 1965).

The equations of motion for the determination of the turbulent secondary flow structure in a non-circular duct can be written as follows (cf. Speziale 1984):

$$\rho\left(\bar{v}_x\frac{\partial \bar{v}_z}{\partial x}+\bar{v}_y\frac{\partial \bar{v}_z}{\partial y}\right) = G+\mu\nabla^2\bar{v}_z+\frac{\partial \tau_{xz}}{\partial x}+\frac{\partial \tau_{yz}}{\partial y}, \tag{53}$$

$$\rho\left(v_x\frac{\partial \bar{\omega}_z}{\partial x}+\bar{v}_y\frac{\partial \bar{\omega}_z}{\partial y}\right) = \mu\nabla^2\bar{\omega}_z+\frac{\partial^2(\tau_{yy}-\tau_{xx})}{\partial x\,\partial y}+\frac{\partial^2\tau_{xy}}{\partial x^2}-\frac{\partial^2\tau_{xy}}{\partial y^2}, \tag{54}$$

$$\nabla^2\bar{\psi} = \bar{\omega}_z, \tag{55}$$

$$\bar{v}_x = -\frac{\partial\bar{\psi}}{\partial y}, \quad \bar{v}_y = \frac{\partial\bar{\psi}}{\partial x}, \tag{56}$$

where

$$\bar{\omega}_z = \frac{\partial \bar{v}_y}{\partial x}-\frac{\partial \bar{v}_x}{\partial y} \tag{57}$$

is the axial mean vorticity, $\bar{\psi}$ is the secondary flow stream function, and G is the constant axial pressure gradient which drives the flow. Of course, (53)–(56) must be solved subject to the no-slip boundary conditions

$$\bar{\boldsymbol{v}} = 0, \quad \bar{\psi} = 0, \quad \boldsymbol{\tau} = 0 \tag{58}$$

on the walls of the duct. These equations of motion are closed once the values of K and l are provided.

A full solution of the equations of motion (53)–(56) coupled with the transport equations for K and l requires a rather substantial computational effort which, unfortunately, is beyond the scope of the present study. Hence, in order to simplify the problem, K and l will be provided empirically and it will be demonstrated computationally that these equations of motion yield a secondary flow consistent with experimental observations. The eddy viscosity

$$\epsilon_{\mathrm{T}} = \tfrac{1}{2}\rho K^{\frac{1}{2}}l \tag{59}$$

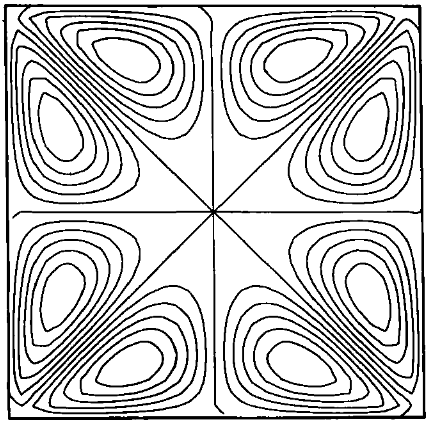

FIGURE 6. Fully developed secondary flow streamlines in a rectangular duct obtained using the nonlinear K–l model.

in turbulent internal flows is known to decrease moderately with an increase in the effective mean shear rate sufficiently far from solid boundaries. A truncated power-law model given by

$$\epsilon_T = \tfrac{1}{2}\rho K_0^{\frac{1}{2}} l_0, \quad S \leqslant S_0, \tag{60}$$

$$\epsilon_T = \tfrac{1}{2}\rho K_0^{\frac{1}{2}} l_0 \left(\frac{S}{S_0}\right)^{n-1}, \quad S \geqslant S_0, \tag{61}$$

where
$$S = (\overline{D}_{ij}\overline{D}_{ij})^{\frac{1}{2}} \tag{62}$$

and K_0 and l_0 are, respectively, some constant reference turbulent kinetic energy and lengthscale (e.g. along the centreline of the duct where the mean velocity gradients vanish) can approximate this behaviour. The lengthscale l in the nonlinear terms in (33) will be approximated by

$$l = l_0, \tag{63}$$

since these terms are of higher-order ((63) constitutes the lowest-order approximation for l). With these approximations, the equations of motion for turbulent duct flow at high Reynolds numbers will be essentially the same as those for a viscoelastic fluid characterized by a second-order Rivlin–Ericksen model with shear thinning (the qualitative similarities between such turbulent secondary flows and viscoelastic secondary flows have long been recognized; see Rivlin 1957). For values of the cut-off shear rate S_0 that are substantially less than its maximum value and for $n \leqslant 0.5$, the idealized power-law model (60)–(62) yields flat velocity profiles in channel flow that are qualitatively similar to figure 1 (cf. Schowalter 1978) and, hence, this substantially simplified model can simulate many of the important features of turbulent flows.

Computations were conducted for this model in a square duct, at extremely high Reynolds numbers, using a finite-difference code developed by Thangam & Speziale (1985) for the analysis of such non-Newtonian flows (this code can be made use of as a result of the analogy discussed above). The secondary flow structure obtained in these computations was relatively insensitive to the values of the constants K_0, l_0, S_0 and n provided that $S_0 \ll S_{\max}$ and $n \leqslant 0.5$. A typical computer-generated contour map for the secondary flow streamlines is shown in figure 6. These computations demonstrated the existence of an eight-vortex secondary flow structure

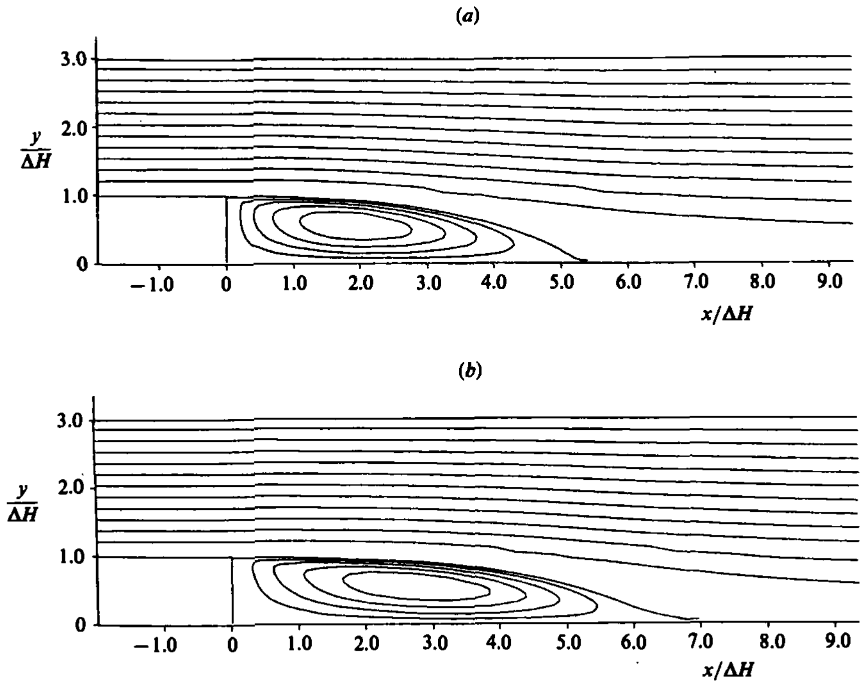

FIGURE 7. Computed streamlines for turbulent flow over a backward-facing step: (*a*) for the linear K–ϵ model; $L/\Delta H \doteq 5.2$; (*b*) for the nonlinear K–ϵ model: $L/\Delta H \doteq 6.7$.

(where momentum is transported towards the corners of the duct) consistent with experimental observations as shown in figure 2. While a detailed computation of the turbulence structure in a rectangular duct predicted by the nonlinear K–l model must await future research, these results are encouraging in that they demonstrate that this model gives rise to a secondary flow with the correct structure. This is in stark contrast to the linear K–l model which erroneously predicts that there are no secondary flows in non-circular ducts.

Finally, it will be demonstrated that the nonlinear K–ϵ model yields considerably improved predictions for separated turbulent flows. It is well known that the linear K–ϵ model badly underpredicts the reattachment point for turbulent flow over a backward-facing step (see figure 3). To be specific, the linear K–ϵ model predicts a separation length $L/\Delta H \doteq 5$ (where $\Delta H = H_2 - H_1$ is the step height), whereas experiments indicate that $L/\Delta H \doteq 7$ as discussed extensively at the 1980–81 AFOSR–HTTM Stanford Conference on Turbulence. Computations were conducted with the nonlinear K–ϵ model derived herein by making use of the TEACH computer code as adapted for the backward-facing-step problem by Chen (1985). The computed streamlines obtained are shown in figure 7 for $H_2/H_1 = 1.5$ and an inlet Reynolds number of approximately 100000. It is clear that the linear K–ϵ model yields a separation length of $L/\Delta H \doteq 5.2$ (see figure 7*a*) whereas the nonlinear K–ϵ model yields a separation length of $L/\Delta H \doteq 6.7$ (see figure 7*b*), which is in much closer agreement with the experimentally observed value of 7. Since both of the computed results shown in figure 7 were obtained using the same transport equations for K and ϵ (which are of the form of (13)–(14)), it would appear that the nonlinear model can yield improved predictions for separated turbulent flows.

5. Conclusion

A nonlinear K–l and K–ϵ model has been developed which constitutes the next highest algebraic approximation (i.e. a quadratic extension of the linear models). This was accomplished by means of an expansion subject to the physical constraints of dimensional and tensorial invariance, realizability, and material frame-indifference in the limit of two-dimensional turbulence. The nonlinear model derived represents a simplified version of a more complex nonlinear eddy-viscosity model obtained by Yoshizawa (1984) using Kraichnan's DIA formalism and has qualitative similarities to the Rivlin–Ericksen fluids of viscoelastic flow. Computations were presented which demonstrated that this nonlinear K–l (and K–ϵ) model, which introduces only one additional independent constant over that which is present in the linear model, yields more accurate predictions for the normal Reynolds stresses in turbulent channel flow. It was also demonstrated computationally that the nonlinear model yields secondary flows of the correct physical form in a square duct (whereas the linear model is fundamentally incapable of doing so) and yields more accurate predictions for separated turbulent flows past a backward-facing step.

Future research is needed to provide a more detailed picture of the turbulence structure in non-circular ducts predicted by this nonlinear K–l and K–ϵ model. In addition, a more detailed quantitative study of the model in a developing turbulent flow with separation should be considered. Some modifications in the transport equations for the turbulent kinetic energy and lengthscale may also be needed and more severe tests of the model should provide useful information in this regard. These more extensive tests of the nonlinear model will be the subject of a future study.

The author would like to thank Dr S. Thangam for his assistance with the turbulent secondary flow computations and Mr Tuan Ngo for his assistance with the turbulent backward-facing-step computations. Thanks are also due to Mr C. Sgouros for his reduction of the turbulent channel flow data which led to the determination of the empirical constants in the nonlinear K–l model, and to Mr N. Hur for drawing most of the figures. This research was supported by the Office of Naval Research under contract no. N00014-85-K-0238 for which Dr Choung Lee served as the project monitor.

REFERENCES

Chapman, S. & Cowling, T. G. 1953 *The Mathematical Theory of Non-Uniform Gases*. Cambridge University Press.

Chen, C. P. 1985 Multiple-scale turbulence closure modelling of confined recirculating flows. *NASA CR* 178536. NASA-Marshall Space Flight Center.

Deardorff, J. W. 1970 A numerical study of three-dimensional turbulent channel flow at large Reynolds numbers. *J. Fluid Mech.* **41**, 453.

Gessner, F. B. & Emery, A. F. 1976 A Reynolds stress model for turbulent corner flows – Part I: Development of the model. *Trans. ASME* I: *J. Fluids Engng* **98**, 261.

Gessner, F. B. & Jones, J. B. 1965 On some aspects of fully-developed turbulent flow in rectangular channels. *J. Fluid Mech.* **23**, 689.

Gessner, F. B. & Po, J. K. 1977 A Reynolds stress model for turbulent corner flows – Part II: Comparisons between theory and experiment. *Trans. ASME* I: *J. Fluids Engng* **99**, 269.

Hanjalic, K. & Launder, B. E. 1972 A Reynolds stress model of turbulence and its application to thin shear flows. *J. Fluid Mech.* **52**, 609.

Hinze, J. O. 1975 *Turbulence*. McGraw-Hill.

HUSSAIN, A. K. M. F. & REYNOLDS, W. C. 1975 Measurements in fully-developed turbulent channel flow. *Trans. ASME* I: *J. Fluids Engng* **97**, 568.

LAUFER, J. 1951 Investigation of turbulent flow in a two-dimensional channel. *NACA TN* 1053.

LAUNDER, B. E., REECE, G. J. & RODI, W. 1975 Progress in the development of a Reynolds stress turbulence closure. *J. Fluid Mech.* **68**, 537.

LAUNDER, B. E. & YING, W. M. 1971 Fully developed turbulent flow in ducts of square cross section. *Rep.* TM/TN/A/11. Imperial College of Science and Technology

LUMLEY, J. L. 1970 Toward a turbulent constitutive relation. *J. Fluid Mech.* **41**, 413.

LUMLEY, J. L. 1978 Computational modeling of turbulent flows. *Adv. Appl. Mech.* **18**, 123.

MELLOR, G. L. & HERRING, H. J. 1973 A survey of the mean turbulent field closure models. *AIAA J.* **11**, 590.

MOIN, P. & KIM, J. 1982 Numerical investigation of turbulent channel flow. *J. Fluid Mech.* **118**, 341.

RIVLIN, R. S. 1957 The relation between the flow of non-Newtonian fluids and turbulent Newtonian fluids. *Q. Appl. Maths* **15**, 212.

RODI, W. 1982 Example of turbulence models for incompressible flows. *AIAA J.* **20**, 872.

SAFFMAN, P. G. 1977 Results of a two-equation model for turbulent flows and development of a relaxation stress model for application to straining and rotating flows. In *Project SQUID Workshop on Turbulence in Internal Flows* (ed. S. Murthy), p. 191. Hemisphere.

SCHOWALTER, W. R. 1978 *Mechanics of Non-Newtonian Fluids*. Pergamon.

SPEZIALE, C. G. 1981 Some interesting properties of two-dimensional turbulence. *Phys. Fluids* **24**, 1425.

SPEZIALE, C. G. 1982 On turbulent secondary flows in pipes of non-circular cross-section. *Intl J. Engng Sci.* **20**, 863.

SPEZIALE, C. G. 1983 Closure models for rotating two-dimensional turbulence. *Geophys. Astrophys. Fluid Dyn.* **23**, 69.

SPEZIALE, C. G. 1984 On the origin of turbulent secondary flows in non-circular ducts. In *Computation of Internal Flows: Methods and Applications, ASME FED 14*, p. 101. ASME.

SPEZIALE, C. G. 1985 Modeling the pressure gradient–velocity correlation of turbulence. *Phys. Fluids* **28**, 69.

THANGAM, S. & SPEZIALE, C. G. 1985 Numerical study of non-Newtonian secondary flows in rectangular ducts. *Tech. Rep.* ME-RT-85035. Stevens Institute of Technology.

TRUESDELL, C. & NOLL, W. 1965 The nonlinear field theories of mechanics. In *Handbuch der Physik*, vol. III/3. Springer.

YOSHIZAWA, A. 1984 Statistical analysis of the deviation of the Reynolds stress from its eddy viscosity representation. *Phys. Fluids* **27**, 1377.